Supplementary Information

Intra-Uterine Calorie Restriction Affects Placental DNA Methylation

RNA extraction

Placental tissues were homogenized in Trizol reagent (Invitrogen, Carlsbad, CA) and total RNA was extracted according to manufacturer's instructions. Briefly, homogenized samples were incubated in room temperature for 5 minutes then 0.2 ml of chloroform per 1ml of Trizol reagent was added and vigorously shaken by hand for 30 seconds. Centrifugation was performed at 12000xg for 15 minutes at 4°C. Aqueous phase of the sample was removed and place it to a new tube. 0.5ml of 100% isopropanol was added to the tube, mixed well, incubated for 10 minutes at room temperature and finally centrifuged at 12000xg for 10 minutes at 4°C. After centrifugation, the supernatent was removed, the pellet was then washed with 75% ethanol, air dried for 15 minutes and dissolved in autoclaved distilled water. The RNA amount was quantified by spectrophotometry.

DNA extraction

The previously snap-frozen murine placental tissues were powdered using a metal pulverizer under dry ice to produce a homogeneous content. A small aliquot of the powdered placenta (25 mg) was treated overnight at 55°C with an extraction buffer (750 μl) that contained proteinase K (200 μg/ml) in 10 mmol of Tris-HCl, 10 mm of EDTA, 50 mm of NaCl and 2% SDS. Following centrifugation at 5 min in room temperature with 10,000 rpm, the separated supernatent was treated with saturated 6 M NaCl solution followed by phenol/chloroform to precipitate DNA which was subsequently purified in 70% ethanol.

PCR identification of the SRY gene

Placental genomic DNA samples (100 ng) were amplified using specific primers for the SRY gene. The forward primer (5' CACTGGCCTTTTCTCCTACC) and reverse primer (5'CATGGCATGCTGTATTGACC) amplified the gene in a 50 μl reaction over 34 cycles with a start temperature of 95°C for 1 min, denaturation at 95°C for 30s, annealing at 50°C for 30s, extension at 72°C for 30s and finally set at 72°C for 5 min. Amplified products were separated by 1% agarose gel electrophoresis and the size of the

ethidium bromide-stained DNA products confirmed in comparison with standard DNA size markers. Amplification of glyceraldehyde-3-phosphate dehydrogenase DNA served as the internal control to confirm integrity of the extracted placental DNA (see Fig 1).

RNA preparation and quantitative real-time PCR (RT-qPCR)

Total RNA was extracted using Trizol reagent (Invitrogen, Carlsbad, CA, USA) according to the manufacturer's instructions. Quantitative and qualitative analyses of isolated RNA were assessed by the ratio of absorbance at 260 and 280 nm and agarose gel electrophoresis. One microgram of total RNA was reverse transcribed to cDNA by reverse transcription (RT) using a SuperScript II Reverse Transcriptase kit (Invitrogen, San Diego, CA) following the manufacturer's instructions. The reverse transcription reaction was performed at 50°C using 5 µg/µl random hexamers. The complementary DNA was employed for quantitative real time pCR by the Taqman assay using Step One plus Real Time PCR System. We used primers and [Tamra~6~Fam] probe for detecting the mRNA level of PEGR1 gene. With regard to *PEGR1*, the 5′-primer was 5′-(TTAACCTGAGCCTAGCGGAT)-3′, the 3′-complementary primer was 3′-(CCAGCGTCATGGAGAAGATA)-5′, and the Fam/Tamra probe was 5′-(ATCGCCTGTTGGCAGCACC)-3′ (Eurofins, MWG Operon). As the house-keeping gene, we used primer and Fam/Tamra probe sets of TaqMan® Rodent 18S rRNA Control Reagents (Product number: 4319413E, Applied Biosystems, Foster City, CA). The thermal cycling conditions included an incubation step for 12 min at 95 °C to denature the UNG enzyme and activate AmpliTaq Gold polymerase, 40 cycles at 95 °C for 30s and 58 °C for 30s . For each reaction, a CT value, which is the number of cycles necessary to reach the threshold, was identified. For quantification of gene expression, we used the standard curve method. CT values were used to read the relative RNA amounts. An mRNA expression value was then obtained by dividing the value for the gene of interest by the value of the *18S*. All samples were run in triplicates.

Sex difference in methylation

We also compared the methylation profiles between genders. In autosomes we observed similar methylation levels between males and females with females having slightly more methylation than males (see Fig S8 for genome wide comparison). This pattern holds for autosomes but not for sex chromosome where the methylation patterns are altered throughout the chromosome, and overall males were slightly more methylated than females (Fig S9), which suggests that this chromosome is under different epigenetic regulation than the autosomes. The higher methylation levels in the male chromosome X are consistent with a recent report on human placentas that observed that hyper methylation of the female inactivated X is mainly found at promoters, while in most other regions, such as inter- and intra-genic loci, it is hypomethylated .

We repeated the same analysis to identify DMRs between female and male groups. In total, we identified 655 and 200 DMRs in autosomes and sex chromosomes, which are associated with 413 and 114 genes, respectively. We observed fewer gene clusters in autosomes (Supplementary file 3), whereas on chromosome X clusters of differential methylation were observed across the entire chromosome (Fig S6, Supplementary File 2). The major network enriched for these differentially methylated genes is associated with embryonic development, cellular function and maintenance, skeletal and muscular system development and function.

RT-qPCR of mir149

Total RNA was extracted using our Trizol reagent (Invitrogen, Carlsbad, CA, USA) and cDNA synthesis was performed using Taqman MicroRNA Reverse transcription kit from Applied Biosystem (, Applied Biosystems, Foster City, CA) with special RT primer set for mir149 (Assay ID 002255). Briefly, RT reactions were performed with 10 ng of total RNA using Multiscribe RT enzyme (50U/μl) with specific mir primers from Applied Biosystem in a thermal cycler at 16°C for 30min, 42°C for 30 min followed by denaturation at 85°C for 5 minutes. The synthesized cDNA was diluted 10-fold before being used for RT-qPCR. The target sequences for miR-29 was UCUGGCUCCGUGUCUUCACUCCC with the PCR primers designed by Applied Biosystem that work with a universal primer targeting the tag that was inserted during RT. The mir 429 was used as the endogenous control. Both the mir429 probe (UAAUACUGUCUGGUAAAACCGU) and primers (Assay ID 001024) were obtained from Applied Biosystems and reverse transcription reaction was done exactly the same way as it was for mir149. The PCR mixture consisted of 10 μl TaqMan Universal PCR master Mix II (no UNG) with mir149 forward and universal reverse primers and cDNA obtained by reverse transcribing10 ng of total RNA. The samples were initially heated at 95°C for 10 min, followed by 40 cycles of 95°C for 15s and 60°C for 60s. The same conditions were used for miR-429 which served as the endogenous control Each RT-qPCR assay was performed in triplicate and the relative miR expression quantified by subtracting the average of quantification cycle (C_q) values from the triplicate reaction of reference control (mir 429). The difference between miR-149 and the internal control provided the difference in C_q value (ΔC_q).

Significance score for enriched gene networks

The IPA application provides a tool for discovery of gene networks within the uploaded gene lists. The IPA application maps each gene identifier to its corresponding gene object in the IPA Knowledge Base. These focus genes are then overlaid onto a global molecular network developed from information contained in the Knowledge Base. Networks of these focus genes are then algorithmically generated based on their connectivity. Each individual IPA network is assigned a significance score (based on p value) representing the likelihood that the focus genes within the network are found therein by random chance. A high number of focus genes within a dataset leads to a higher network score (equal to the negative exponent of the respective p value such that a score of 3 corresponds to a p value of 10E-3). Each of the IPA-derived gene networks provided in the Results section has a significance score of ≥ 15 (i.e. p value ≥ 10E-15) and the gene networks are presented as merges of the top two scoring networks within each of the respective gene lists.

Table S1A: Number of placentas in genome wide DNA methylation analysis

	CR	CON	Total
Female	2	2	4
Male	3	3	6
Total	5	5	10

Table S1B: Number of placentas in genome wide gene expression analysis

	CR	CON	Total
Female	2	2	4
Male	3	3	6
Total	5	5	10

Table S2A: Average methylation level per sample

CG methylation levels (%)	CON					CR				
	male			female		male			female	
Autosomes	35.69	35.09	35.36	34.74	36.41	34.00	34.70	33.90	35.07	34.37
chrX	42.17	39.60	41.42	39.88	41.81	39.32	38.87	38.83	39.80	38.34
chrY	56.96	55.86	56.36	NA	NA	54.29	55.29	54.94	NA	NA
ChrX/Y	42.37	39.82	41.63	39.88	41.81	39.52	39.09	39.05	39.80	38.34
Genome	35.88	35.23	35.55	34.88	36.55	34.16	34.83	34.05	35.19	34.48

Table S2B: Average methylation level per group

CG methylation levels (%)	male CR	male CON	female CR	female CON
Autosomes	34.20	35.38	34.72	35.58
chrX	39.01	41.06	39.07	40.85
chrY	54.84	56.39	NA	NA
Genome	34.35	35.55	34.84	35.72

Table S2C: T-tests for group comparisons

P-value	Autosomes	Sex chromosomes	Genome
CR vs. CON	0.0205*	0.0232*	0.0181*
CR vs. CON (male)	0.0226*	0.1082	0.0194*
CR vs. CON (female)	0.4836	0.2893	0.4736
Female vs. Male	0.5302	0.9351	0.5640

*P-value<0.05

Table S3: Enriched gene networks associated with DMR in chr13 (60-80Mbp)

Enriched gene networks	1. Cell Death, Cancer, Dermatological Diseases and Conditions 2. Cell Morphology, Nervous System Development and Function, Tissue Development 3. Reproductive System Development and Function, Cell Cycle, Reproductive System Disease 4. Cell Death, Cell Cycle, Cell-To-Cell Signaling and Interaction 5. Connective Tissue Disorders, Organismal Injury and Abnormalities, Cell Morphology
Associated diseases and disorders	1. Developmental Disorder 2. Genetic Disorder 3. Neurological Disease 4. Skeletal and Muscular Disorders 5. Cancer

Table S4: Number of differentially methylated genes

	Genes with up-regulated DMR	Genes with down-regulated DMR	Overlap (genes with both up- and down-regulated DMR)	Total
CR vs. CON	131	168	2	297
CR vs. CON (sex effect)	309	380	22	667
CR vs. CON (male)	175	308	6	477
CR vs. CON (female)	187	280	8	459
Female vs. Male (autosomes)	156	264	7	413
Female vs. Male (chr X/Y)	53	63	2	114

Table S5: Primers used for bisulfite sequencing

DMR	Name	Sequence

1	Forward primer JP10383	`5'-AGCCTGTTTGGTGTCCAGGGGAC-3'`
		`5'-AGTTTGTTTGGTGTTTAGGGGAT-3'`
		`23bp and Tm 54.8°C`

	Reverse primer JP10384	`5'-TTCCTGCACATATATTTTTCCATGATGCAGGAAAATGAGC-3'`
		`5'-TTCCTACACATATATTTTTCCATAATACAAAAAAATAAAC-3'`
		`40bp and Tm 54.9°C`

2	Forward primer JP10385	`5'-GGAACTCCCCTGCTTCCATACACAGCTGTAGGCAGAAAC-3'`
		`5'-GGAATTTTTTTGTTTTTATATATAGTTGTAGGTAGAAAT-3'`
		`39bp and Tm 54.5°C`

	Reverse primer JP10386	`5'-TGTCTGATCACAGAAATAAAGCCGACCATATTGTC-3'(partial repeat)`
		`5'-TATCTAATCACAAAAATAAAACCRACCATATTATC-3'`
		`35bp and Tm 53.6 to 54.6°C`

3	Forward primer JP10387	`5'-GCCAGAAGCGGTATTGGGAACTGTC-3'`
		`5'-GTTAGAAGYGGTATTGGGAATTGTT-3'`
		`25bp and Tm 53.4 to 55.6°C`

	Reverse primer JP10388	`5'-GCTTGATGGGCAGAGGGCTGCCAAGCTGTTATCTTTGC-3'`
		`5'-ACTTAATAAACAAAAAACTACCAAACTATTATCTTTAC-3'`
		`38bp and Tm 54.3°C`

Table S6: Enriched gene functions in differentially methylated genes

Comparison	Enriched gene ontology (p<0.05)
CR vs. CON	calcium ion binding, biological adhesion, cell fraction, passive transmembrane transporter activity, DNA/RNA helicase, C-terminal, learning, cytoplasmic vesicle, cell morphogenesis involved in neuron differentiation, lipid binding, regulation of neuron apoptosis, behavior, Pleckstrin homology, fatty acid metabolic process
CR vs. CON (differential sex effect)	homeobox, transcription factor activity, embryonic morphogenesis, neuron differentiation, embryonic skeletal system development, limb development, appendage development, skeletal system development, embryonic organ morphogenesis, regulation of RNA metabolic process, hemopoietic or lymphoid organ development, growth, immune system development, heart morphogenesis, muscle tissue development, heart growth, blood vessel remodeling, negative regulation of macromolecule metabolic process
CR vs. CON (female)	calcium channel complex, voltage-gated calcium channel complex, voltage-gated calcium channel complex, cell junction, calcium channel activity, cell projection organization, long-term depression, insulin signaling pathway, arrhythmogenic right ventricular cardiomyopathy (ARVC), cell morphogenesis, wnt receptor signaling pathway, lipid binding, adult locomotory behavior
CR vs. CON (male)	skeletal system development, calcium ion binding, chordate embryonic development, pathways in cancer, regulation of mesenchymal cell proliferation, tube morphogenesis, transcription factor activity, embryonic organ development, embryonic skeletal system morphogenesis, sodium channel activity, bone development, cell differentiation in spinal cord, lipid localization, ensheathment of neurons, lipid transport, lipid transport, motor activity, neuron projection morphogenesis, pancreas development, sex determination
Female vs. Male	biological adhesion, cell-cell adhesion, developmental protein, cytoskeleton, type II diabetes mellitus, insulin signaling pathway, differentiation, regulation of cytoskeleton organization, visual behavior,sphingolipid metabolism, central nervous system neuron development

Table S7: Differentially methylated MicroRNAs

	Gene ID	DMR	Enriched functions in the regulated targets
1	Mir149	diet-male, diet	positive regulation of macromolecule metabolic process; positive regulation of nitrogen compound metabolic process
2	Mir1186	diet	NA
3	Mir711	diet-female	NA
4	Mir196a-1	diet-female	skeletal system morphogenesis, Homeobox, embryonic organ morphogenesis, embryonic organ development, developmental protein
5	Mir1224	diet-female	metal-binding, cytoplasmic vesicle, neuromuscular process, transcription regulation
6	Mir199b	diet-sex-effect, diet-female	hormone secretion, Endocytosis, endoplasmic reticulum, regulation of nucleobase, nucleoside, nucleotide and nucleic acid metabolic process
7	Mir1981	diet-male	NA
8	Mir1948	diet-male	NA
9	Mir196b	diet-sex-effect	chromosomal rearrangement, Homeobox protein, antennapedia type, conserved site, nucleoside-triphosphatase regulator activity, skeletal system morphogenesis, regulation of nucleobase, nucleoside, nucleotide and nucleic acid metabolic process
10	Mir335	sex	steroid hormone receptor signaling pathway, transcription regulation, metal ion binding
11	Mir1966	sex	NA
12	Mir148a	sex	establishment of protein localization, regulation of nitrogen compound metabolic process, regulation of transcription, vesicle-mediated transport
13	Mir92-2	sex	NA
14	Mir106a	sex	Melanoma, interphase of mitotic cell cycle, induction of programmed cell death, regulation of apoptosis, regulation of cell size
15	Mir363	sex	activator, regulation of transcription,neuron projection
16	Mir19b-2	sex	NA
17	Mir2137	sex	NA
18	Mir18b	sex	NA
19	Mir20b	sex	NA

Table S8: The weight of embryos and placentae

Group	CON			CR		
Weight (gram)	Embryo	Placenta		Embryo	Placenta	
	1.00	0.09	male	0.51	0.06	male
	0.90	0.10	male	0.56	0.06	male
	1.10	0.10	male	0.62	0.05	male
	0.80	0.06	female	0.43	0.07	female
	0.81	0.08	female	0.45	0.07	female
Average weight (SE)	0.922 (0.0573)	0.086 (0.0074)		0.514 (0.0350)	0.062 (0.0037)	

Table S9: Criteria for DMR

Comparison	Δ methylarion level	Z score	Estimated FDR
CR vs. CON	0.15	2	4.75%
CR vs. CON (sex effect)*	0.075	3.95	4.03%
CR vs. CON (male)	0.15	2	4.21%
CR vs. CON (female)	0.15	2	4.88%
Female vs. Male (autosome)	0.15	2	4.43%
Female vs. Male (chr X/Y)	0.15	2	4.03%

*: the calculation of t-scores (which Z score is based on) and the Δ methylation level is different on this test (see Methods), so the threshold is chosen differently from the others.
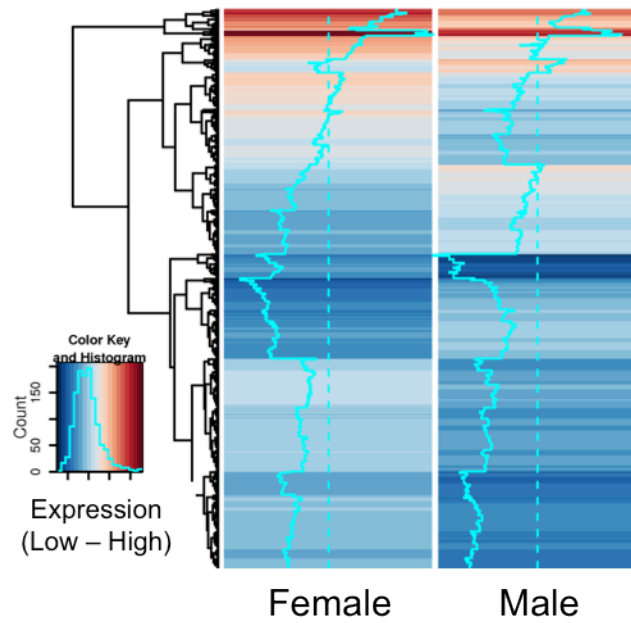
Figure S1: Heatmap of gene expression levels between female and male
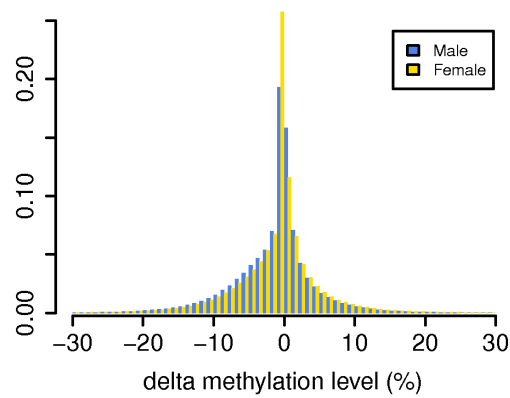
Figure S1: Histogram of Δ methylation levels between CR and CON
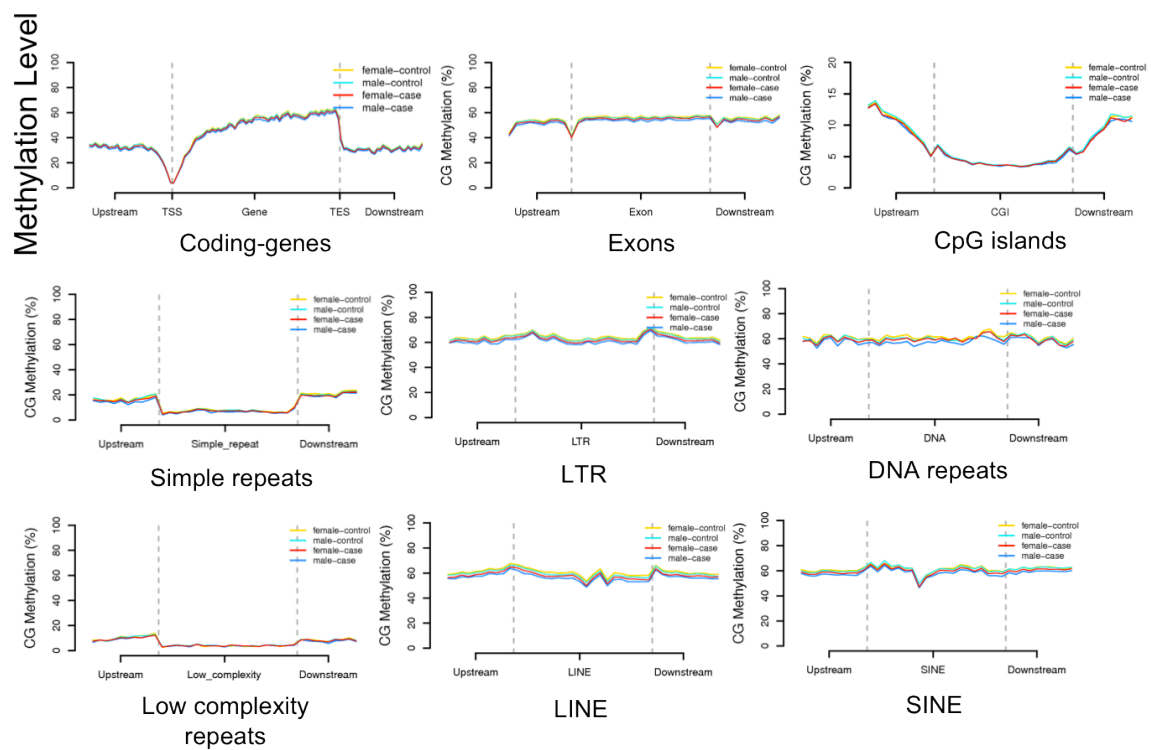
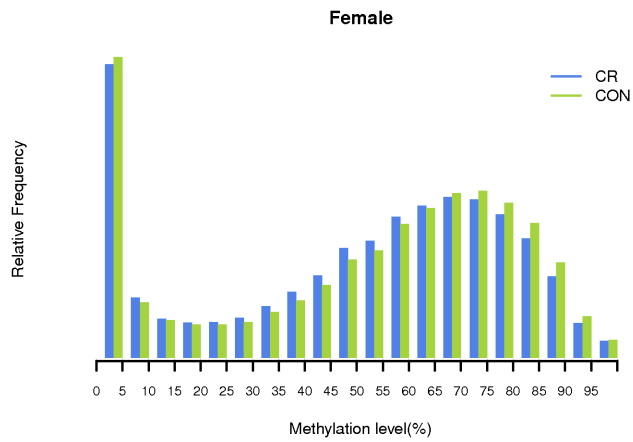**Figure S2: Metaplots of coding genes, exons, CpG islands, and repetitive sequences in different class**

A.

Male

B.
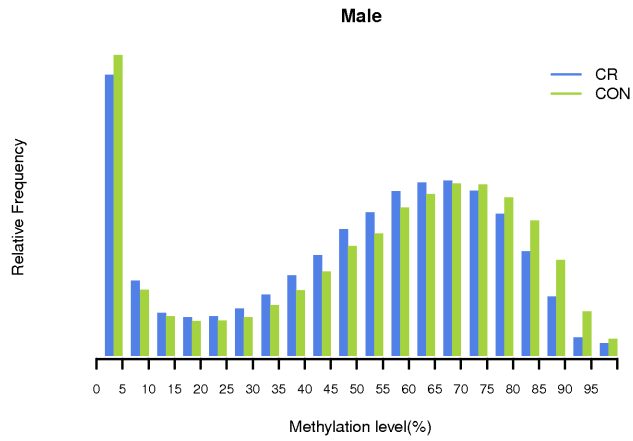
Female

Figure S3: Distribution of methylation levels in RRBS fragments; CR vs. CON in A. males and in B. females.

region3-male-CR (52.91%)   region4-male-CR (46.83%)   Region4-RRBS-male-CR (83.58%)

region3-male-CON (54.37%)   region4-male-CON (36.11%)   Region4-RRBS-male-CON (12.43%)

Number of sequences

DMR2   DMR3   DMR3
chr4:155510877-155510994   chr7:135831560-135831733   chr7:135831560-135831733
(Traditional BS Sequencing) (Traditional BS Sequencing)   (RRBS)

Individual CG sites
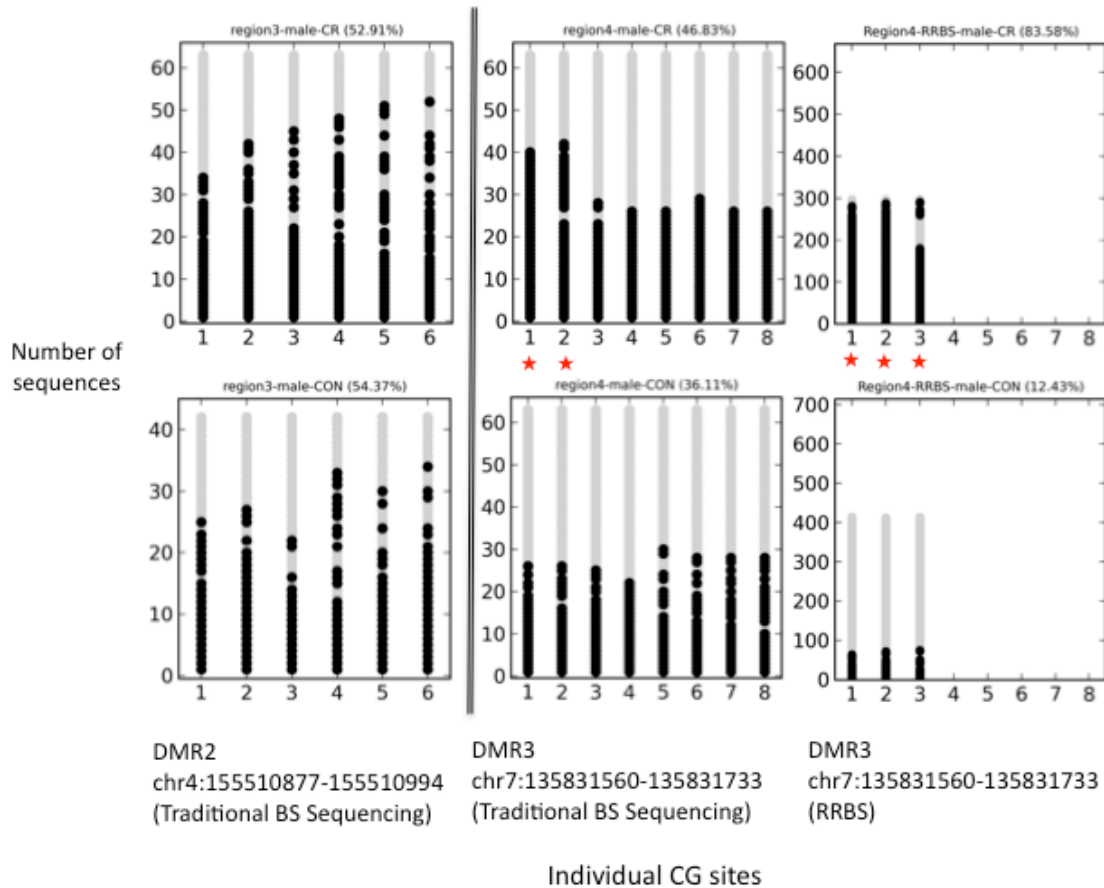
Figure S4 DMR validation traditional bisulfite sequencing.
Bubble plots show the sequences from the traditional bisulfite sequencing, aligned to the 2 predicted by RRBS (DMR2 and DMR3). Each row shows the methylation status of the individual CpG sites within the DMR (black and gray circles stand for methylated and unmethylated cytosines). The average methylation levels are in the brackets. Red *: p-value<0.05, Binomial test of differential methylation per site between CR and CON.
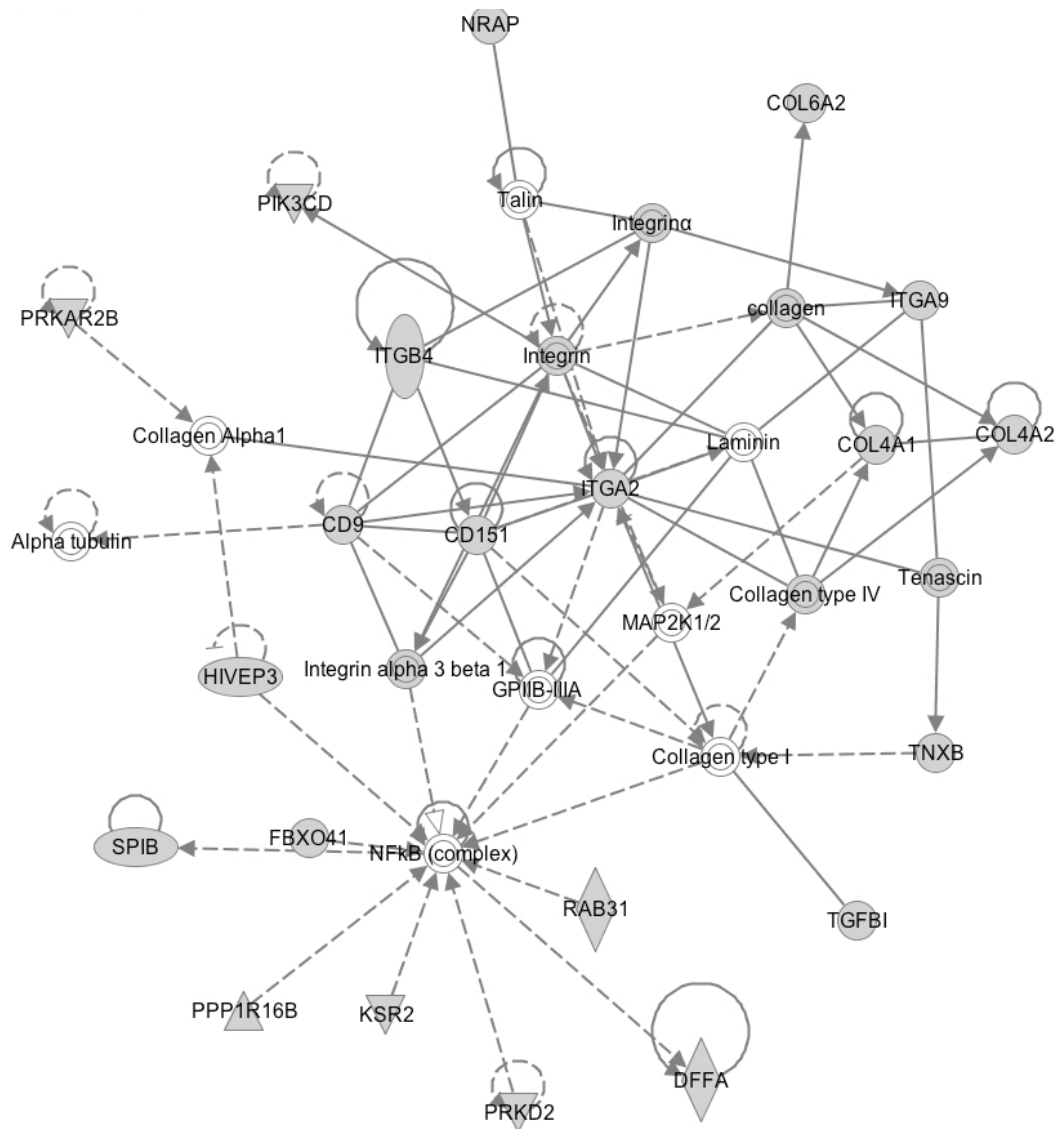
Figure S5: A major network enriched with 21 differentially methylated genes (shaded) with functions of Cardiovascular System Development and Function, Cellular Movement, Embryonic Development

CR vs. CON
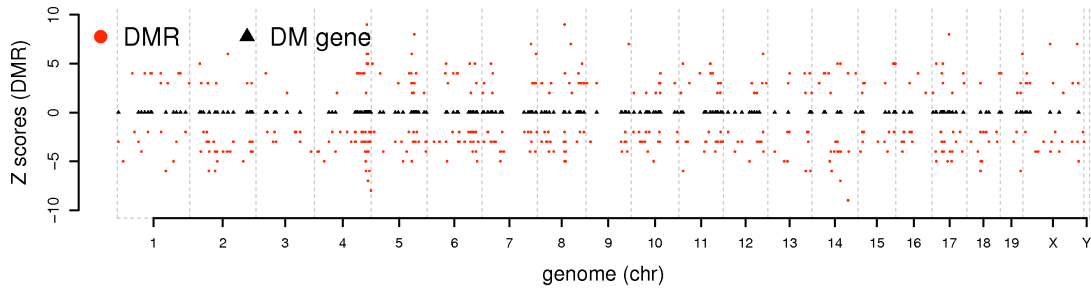
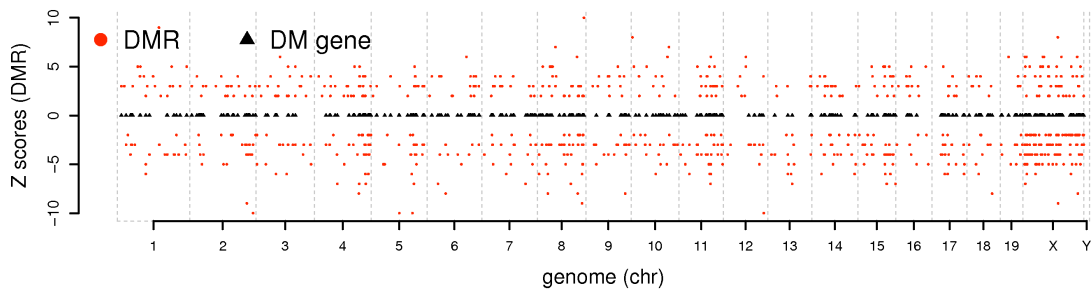

CR vs. CON (sex effect)
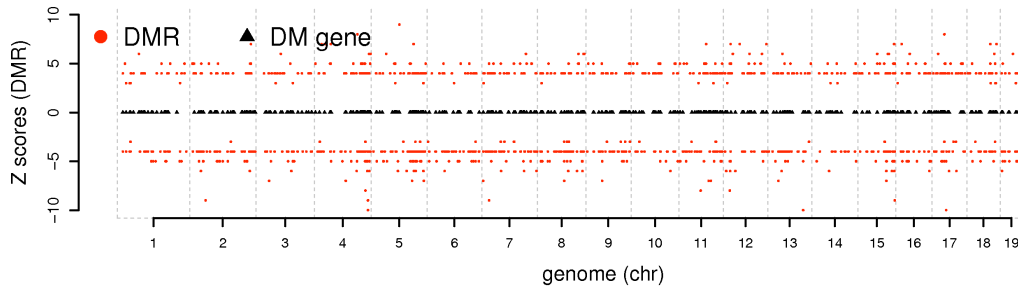
Female vs. Male

Figure S6. Genome wide views of differentially methylated fragments and the associated genes

Red circles are DMR with the z-scores in y axis, black squares are the differentially methylated genes associated to DMR;
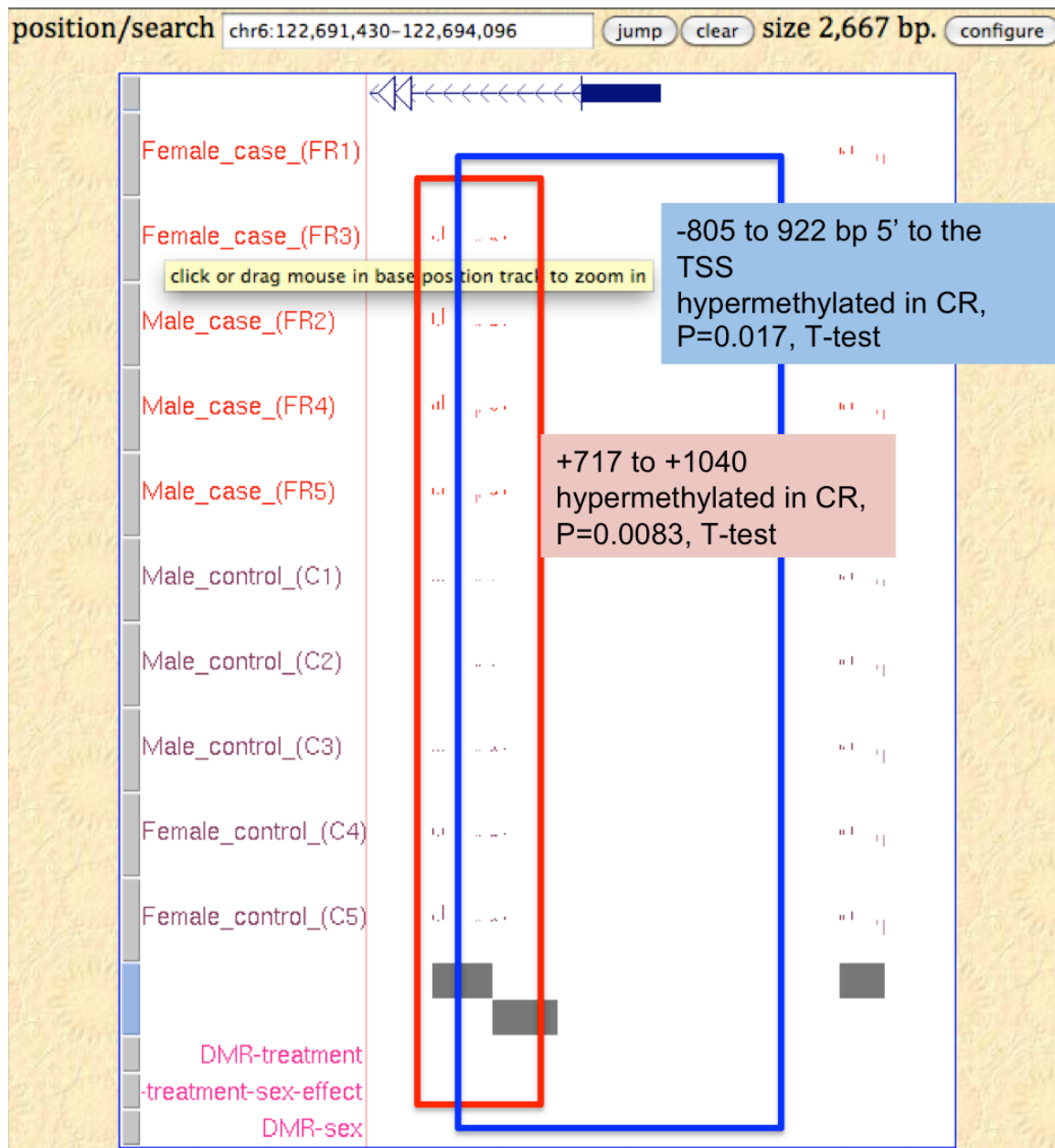
Figure S7 Screenshot of methylation levels at Glut3; The CpG cluster is marked for investigation of differential methylation
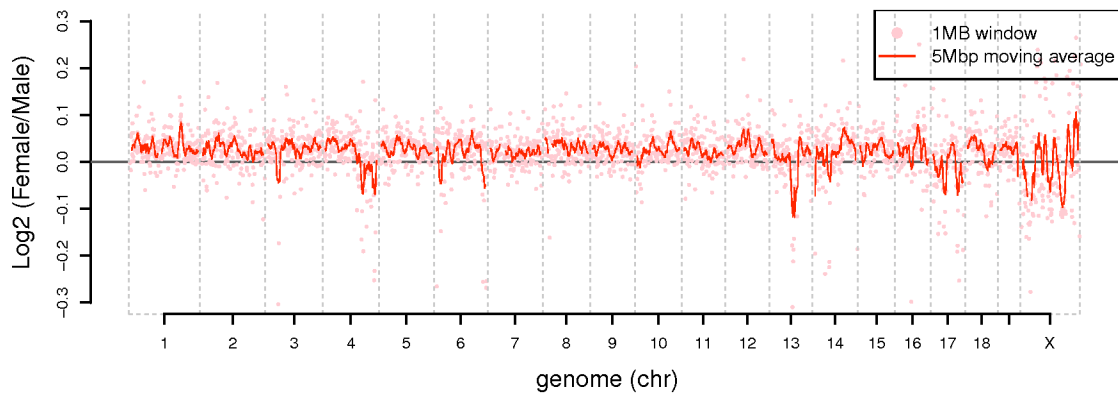
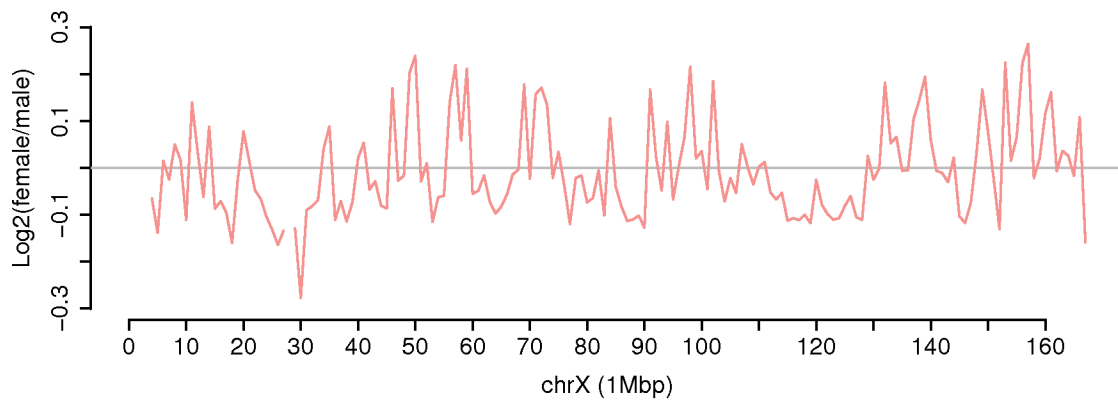**Figure S8:** Comparison of methylation levels between females and males

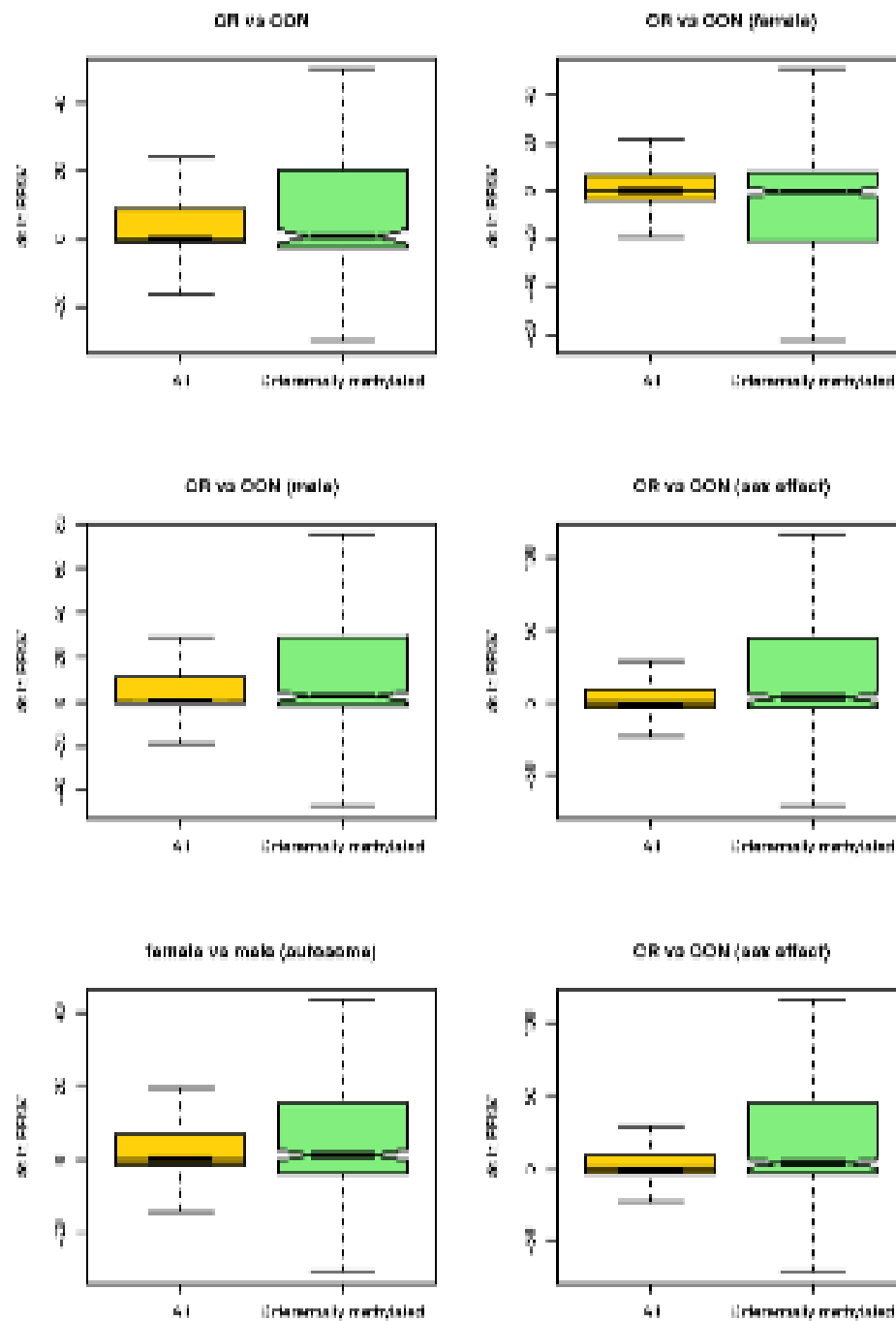**Figure S9:** Comparison of methylation levels between females and males in X chromosome

Figure S10: Boxplots of changes of expression levels in differentially methylated genes
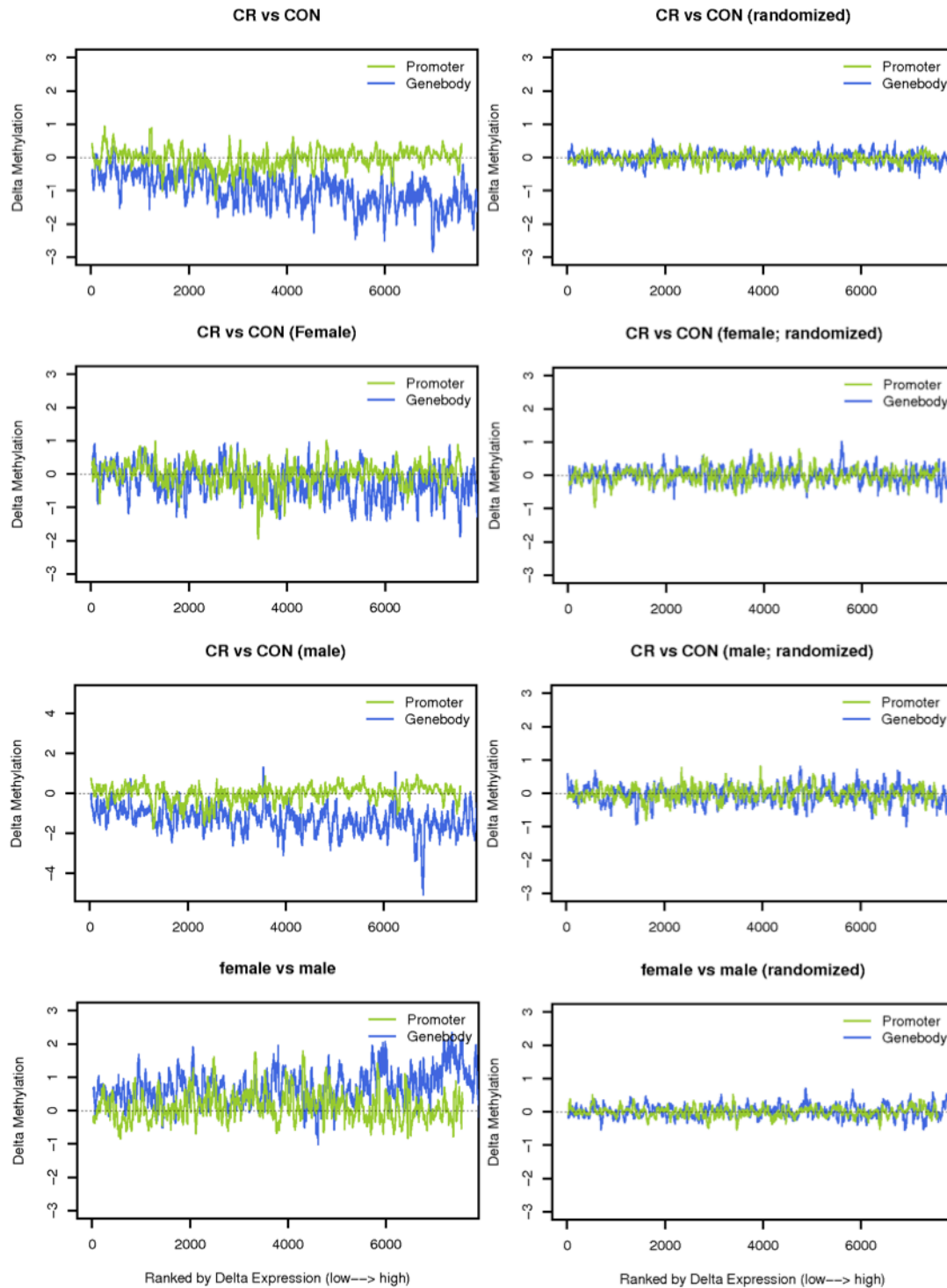
Figure S11: Changes of methylation levels in promoters and genes ranked by the change in gene expression level. The left-hand figures show the change of methylation level in diffeent comparisons. The right-hand figures are from simulated methylomes with the same methylation level.